Turbulent Base Flow on an Axisymmetric Body with a Single Exhaust Jet

R. J. Dixon*
The Boeing Company, Seattle, Wash.

AND

J. M. Richardson†
TRW Systems Group, Houston, Texas

AND

R. H. Page‡
Rutgers—The State University, New Brunswick, N. J.

Korst's two-stream theoretical base flow analysis is extended to treat base flow on an axisymmetric afterbody with a single operating exhaust nozzle. The flow around the afterbody and in the jet is supersonic with turbulent axisymmetric mixing occurring along the separated flow boundaries. The pressure in the base separated region increases in the downstream direction and is constant in a radial direction. A complete description of the base flow is obtained from the analysis permitting the prediction of base pressure and other flow parameters of interest. The analysis is shown to agree with experimental data. The results obtained from a parametric study performed with the analysis illustrate the influence on base drag of some of the significant geometric and operating parameters.

Nomenclature

A = area
C = Crocco number
C_D = drag coefficient
c_p = specific heat at constant pressure
D = diameter
g_c = conversion factor
G = mass bleed rate
M = Mach number
P,q = pressure and dynamic pressure, respectively
R = cylindrical radius
$\mathcal{R}$ = gas constant
$\Re$ = mixing layer reference streamline
T = temperature
u = velocity
X,Y = reference coordinates
x,y = instrinsic coordinates
$\bar{x},\bar{y}$ = Mangler coordinates
β = dummy variable
γ = ratio of specific heats
δ^* = displacement thickness
ϵ = nozzle expansion ratio, A'_1/A_t
σ = mixing layer similarity parameter
η = similarity coordinate
ρ = density
θ = flow angle
ϕ = velocity ratio, u/u_a

Subscripts

a = inviscid flow adjacent to the mixing layer
B,b = base and base region, respectively
c = nozzle chamber
d,j = discriminating and jet boundary streamlines, respectively
m = coordinate shift
o = stagnation conditions
t = nozzle throat
w = wall
∞ = freestream
1,2,3,4 = regions of the base flowfield, Fig. 1

Superscript

$( )'$ = exhaust nozzle (jet) flow

Presented as Paper 69-650 at the AIAA Fluid and Plasma Dynamics Conference, San Francisco, Calif., June 16–18, 1969; submitted July 1, 1969; revision received January 26, 1970. The authors gratefully acknowledge the contributions of F. A. Gruenich and B. E. Wetzel for their efforts in the development of the present analysis.

* Research Specialist, Aerospace Group.
† Staff Engineer, Power Systems Department.
‡ Chairman Department of Mechanical and Aerospace Engineering.

Introduction

THE force acting to retard the flight of a thrusting axisymmetric body, exclusive of fins or other protuberances projecting into the airstream, consists primarily of wave, friction, and base drag. The designer wishes to eliminate or minimize these retarding forces. Friction drag is the least amenable to change, since it is essentially a function of the total surface area exposed to the airstream and the local Reynolds number, but wave drag and base drag are strong functions of the configuration. It is usually not possible to completely eliminate base area on a missile because of the necessity to accommodate the propulsion system and other related equipment in the base region. The external airstream separates from the body at the base and converges toward the axis of symmetry, causing the flow to expand to a $P < P_\infty$. The resulting low base pressure P_b can account for a significant portion of the total vehicle drag. This paper describes an analytical solution for the base component of the total drag for an axisymmetric supersonic body with a supersonic exhaust jet under turbulent flow conditions.

The designer of flight vehicles is usually required to establish his development test configuration before his final design has evolved. As a result, test data are collected on a configuration similar to, but not necessarily the same as, the final configuration. For power-on base flow, testing is com-

plicated by the problems encountered in simulating the engine exhaust jet. Testing of this type is both costly and time consuming. In preliminary design studies it is usually not possible or practical to test all of the configurations of interest over the entire vehicle operating range. To plan an efficient test program, to perform meaningful design trade studies, and to scale off-design data to design conditions requires the use of a comprehensive flow analysis.

The mechanics of base flowfields have received considerable attention, but only recently have satisfactory analytical solutions for base flows become available. Excellent reviews of the current status of this work have been given by Sedney,[1] Przirembel,[2] and Hong.[3] Most of the work cited relates to flow on two-dimensional bodies or on unpowered axisymmetric bodies. In comparison, little analytic work has been done treating the problem of base flow on an axisymmetric thrusting body because of the complications which are added by the presence of the jet exhaust flow. Most of the effort associated with power-on base flow has been directed at experimental investigations. In the survey by Redeker,[4] data were found covering the Mach number range from 0 to 11. The work reported by Baughman and Kochendorfer[5] and Beheim, Klann, and Yeager[6] and their included references are excellent examples of the detailed experimental studies which have been conducted for power-on base flow.

The theoretical analysis of the complex flowfield generated by the interaction of the jet exhaust with the external flow for a thrusting supersonic vehicle has become feasible with the development of large computers. The analyses that have been formulated to date have been primarily extensions of Korst's[7] two-dimensional base flow theory. The validity of Korst's treatment of base-separated flows has been verified for a wide range of conditions (for example, see Kessler[9]). Korst's concept of the discrimination and jet boundary streamlines is one of the key elements in the success of this approach. Korst and Tripp[8] extended the single-stream analysis to treat the two-stream interaction problem. This interaction model has been applied to bodies with jet flow issuing from the base.[5,6,10,11] The agreement with experimental data obtained from these analyses establishes the validity of this approach for the power-on base flow problem.

Analysis

The solution of the base flow on an axisymmetric body with a single exhaust jet presented in this paper is based on the Korst base flow theory.[7,10] The flowfield is divided into components that are analyzed separately. These separate analyses are then combined. Figure 1 shows one-half of the axisymmetric flowfield. Although the flowfield has been simplified, it contains all of the elements necessary to quantitatively assess the base flow. The external flow conditions at region 1 are assumed to be known. Between regions 1 and 2, the freestream flow expands or compresses to P_b. Mixing of the adjacent inviscid flow and the "recirculation" region occurs between regions 2 and 3. Finally realignment of the body flow to the jet flow occurs by recompression between regions 3 and 4. The jet exhaust flow components, indicated with primes, are similar to the external flow.

The occurrence of either an expansion or compression from region 1 to 2 (or 1′ to 2′) is dependent on level of P_b in comparison to P_1 (or P'_1). A compression can occur either in the external flow or the jet flow, but not in both at the same time. Detailed mixing layer profiles (velocity, temperature, and density) are required to determine mass, momentum, and energy transport in the base region and to determine an escape criteria for the mixing layer flow. The specific locations of the mixing layer profiles are determined by integral methods using mass, momentum, and energy conservation. The pressure in the recirculation region is allowed to vary in an axial direction, but it is assumed constant in a radial direction. The pressure after recompression in regions 4 and 4′ is equal along the slip surface.

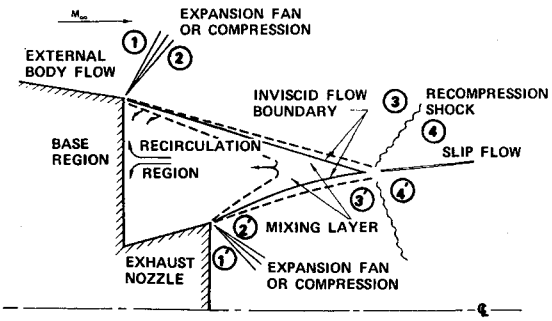

Fig. 1 Single nozzle base flowfield.

The flow model enables the pressures, Mach numbers, and turning angles to be determined as functions of the initial flow conditions at regions 1 and 1′. Mass bleed either into or out of the base region may also be taken into account. Two limiting conditions considered in the analysis are 1) the jet flow impinges on an outer skirt or shroud, and 2) the nozzle is so long that external flow impinges on the nozzle wall. These limiting cases are similar to the supersonic ejector and the sting-mounted-body problems.

Inviscid Flow

For completely supersonic and adiabatic flows, the method of characteristics provides an exact numerical solution for the inviscid flowfield. Solutions for both the external and internal flowfields are obtained numerically, using a solution of the rotational characteristics equations formulated by Eastman.[12–14] The external flowfield is calculated for a real gas using partition functions for the thermodynamic properties.[15] The boundary condition employed for this calculation specifies that the edge of the external inviscid flowfield remains linear after initially adjusting to P_b. This assumption results in an axial pressure gradient through the recirculation region. The shape of the internal inviscid flowfield (plume) is computed for an ideal gas using the axial pressure distribution determined from the external flow calculation as a boundary condition.

The usual assumption of constant P_b throughout the recirculation region is not employed herein, because initial calculations for the inviscid flow with this assumption resulted in recompression region pressures that did not agree with experimental data. Figure 2 shows the $P_w(X)$ obtained by Beheim[16] on the sting of an axisymmetric body. For stings of three different diameters, we found that the in-

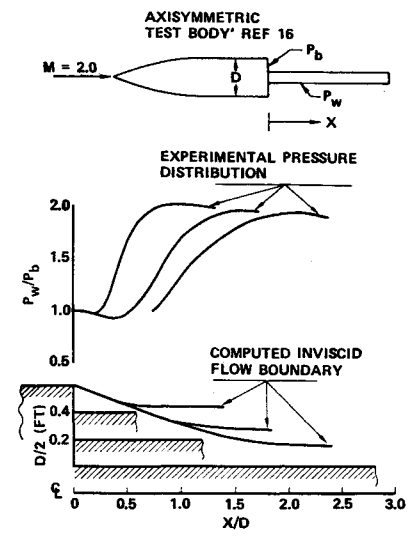

Fig. 2 Method-of-characteristics solution for base region.

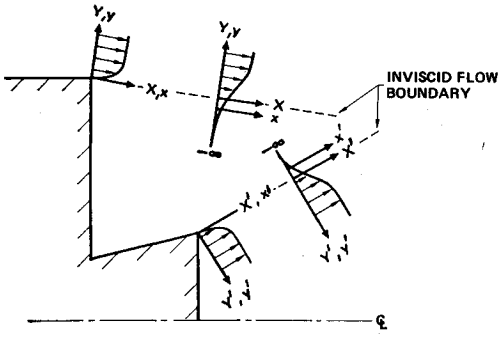

Fig. 3 Mixing layer coordinate system.

viscid flow boundary was initially straight and then tended to approach asymptotically the direction of the sting. The data presented by other investigators support this conclusion.[2,3,17,18]

Flow properties along a starting line must be known for both the external and internal flows. A radial starting line located at the body base is generally specified for the external flow, while flow properties across the nozzle exit plane are nominally used for the internal flowfield. With the initial conditions specified, assuming a value for P_b will permit the calculation of the entire inviscid flow in the base region.

Mixing Layer

The mixing layer solution employed is based on the Page[19] extension of isoenergetic two-dimensional turbulent mixing to nonisoenergetic mixing layers. Fully developed mixing profiles are assumed, so that the effect of the initial boundary layer is neglected. This so-called restricted mixing theory[7] results in the calculation of the minimum base pressure[9] and therefore, is conservative from the standpoint of drag prediction. The coordinate systems employed are 1) the reference system (X,Y), and 2) the intrinsic system (x,y) (Fig. 3). The former is aligned with the inviscid jet and body flowfields; the latter is inherent to the jet and body mixing layer solutions and is shifted from the reference system. The origins of both systems are located at the point of flow separation, i.e., the beginning of the mixing layer.

The velocity profile in the mixing layer is presented by

$$\frac{u}{u_a} \equiv \phi = \frac{1 + \text{erf}\eta}{2} = \frac{1}{2} + \frac{1}{\pi^{1/2}} \int_0^n e^{-\beta^2} d\beta \qquad (1)$$

Korst[24] has shown that Eq. (1) satisfies the initial and boundary conditions for a two-dimensional turbulent free mixing layer with a negligible initial boundary layer. This solution has been applied to the axisymmetric mixing layers considered in the present analysis by employing the Mangler transformation,[25] which reduces the boundary-layer equations in axisymmetric flow to two-dimensional form when the flow radius is large compared to the viscous thickness. The initial and boundary conditions for the two-dimensional solution apply to the transformed equations, so that the solution is similar.

The similarity coordinate η defined in terms of the Mangler transform becomes

$$\eta = \sigma\bar{y}/\bar{x} \qquad (2)$$

where $\bar{x},\bar{y}$ are the Mangler coordinates defined by

$$\bar{x} = \int_0^x \left[\frac{R_o(x)}{R_B}\right]^2 dx, \quad \bar{y} = \frac{R_o(x)}{R_B} y \qquad (3)$$

and $R_o(x)$ is the inviscid flow radius and R_B (or R'_B) is a reference length. For the external mixing region R_B is the body base radius, and for the exhaust jet mixing region R'_B, the jet exit radius, is used.

The total temperature ratio, T_o/T_{oa}, is obtained from Crocco's integral of the boundary-layer equations applied to the mixing region[19]

$$T_o/T_{oa} = (1 - \phi)T_b/T_{oa} + \phi \qquad (4)$$

T_b is the temperature of the gas in the recirculation region at a point where the velocity is zero.

The turbulent mixing similarity parameter σ employed in Eq. (2) is the only empirical quantity that must be known to calculate the base flowfield. There is some disagreement among the various investigators on the compressibility correction for σ.[8,20,21,22] For this analysis, the relationship suggested by Tripp[8] is used:

$$\sigma = 12 + 2.758M_a \qquad (5)$$

This relationship is in reasonable agreement with the available data. For gases other than air, the relationship suggested by Page[23] is used;

$$\sigma = 12 + 6.16[C_a^2/(1 - C_a^2)]^{1/2} \qquad (6)$$

This formulation of σ is equal to Eq. (5) defined in terms of the Crocco number.

The velocity distribution, Eq. (1), is obtained from a linearized solution of the equation of motion. The location of the profile is adjusted to represent more closely the solution of the complete equation. Equation (1) is assumed to apply in the intrinsic coordinate system. This coordinate is assumed to be shifted relative to the physical system so that

$$X = x, \; Y = y - y_m(x), \; y_m(0) = 0$$

The coordinate shift y_m is determined by requiring the momentum in the inviscid flow to equal that in the mixing layer. At a given axial location, momentum conservation for the mixing layer is expressed as

$$\int_0^{\mathfrak{R}} \rho_a u_a^2 R dY \Big|_X = \int_{-\infty}^{\mathfrak{R}} \rho u^2 R dY \Big|_X \qquad (7)$$

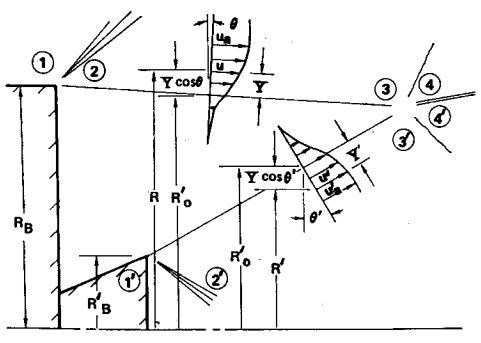

Fig. 4 Geometrical relationship between radii and mixing region coordinates.

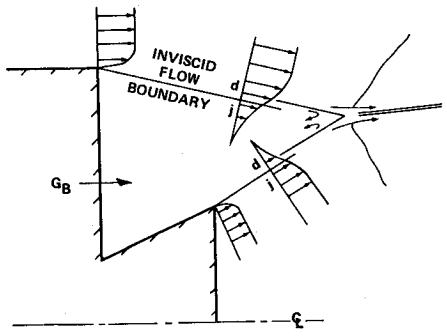

Fig. 5 Base region mass balance.

where as shown in Fig. 4,

$$R = R_o + Y\cos\theta \tag{8}$$

The upper limit of integration $\mathfrak{R}$ is a reference streamline in the inviscid flow outside the mixing region. Rewriting Eqs. (7) and (8) in terms of η results in

$$\int_{\eta_m}^{\eta_{\mathfrak{R}}} Rd\eta = \int_{\eta_{-\infty}}^{\eta_{\mathfrak{R}}} \frac{(1 - C_a^2)\phi^2 R}{T_o/T_{oa} - C_a^2\phi^2}\, d\eta \tag{7a}$$

$$R = R_o + (R_B\bar{x}/R_o\sigma)(\eta - \eta_m) \tag{8a}$$

The density ratio ρ/ρ_a in Eq. (7) has been determined assuming a perfect gas from the relationship

$$\rho/\rho_a = (1 - C_a^2)/(T_o/T_{oa} - C_a^2\phi^2) \tag{9}$$

where C_a is the Crocco number of the inviscid flow,

$$C_a = u_a/(2c_pT_{oa})^{1/2} \tag{10}$$

The only unknown in Eq. (7a) is η_m, which appears both as a limit of integration and in the expression for R, hence η_m can be determined by trial and error.

The shift of the velocity profile, η'_m, for the exhaust jet mixing layer is determined by a procedure similar to that outlined for η_m, with the exception that R' is defined by

$$R' = R'_o - Y'\cos\theta' \tag{11}$$

so that the equation corresponding to Eq. (8a) becomes

$$R' = R'_o - [R'_B\bar{x}'/R_o\sigma'](\eta' - \eta'_m)\cos\theta' \tag{11a}$$

To locate the mixing layer jet boundary streamline Yj, which separates the mass originally in the inviscid flow from the mass entrained into the mixing layer, we apply mass conservation to the mixing layer. In the reference coordinate system,

$$\int_o^{\mathfrak{R}} \rho_a u_a R dY\Big|_X = \int_j^{\mathfrak{R}} \rho u R dY\Big|_X \tag{12}$$

Transformed in terms of η, Eq. (12) becomes

$$\int_{\eta_m}^{\eta_{\mathfrak{R}}} Rd\eta = \int_{\eta_j}^{\eta_{\mathfrak{R}}} \frac{(1 - C_a^2)\phi R}{T_o/T_{oa} - C_a^2\phi^2}\, d\eta \tag{12a}$$

which can be solved for η_j once η_m is determined.

Recompression Region

The recompression region is the final component of the base flowfield. Since the pressure in the recirculation region is assumed to be constant in a radial direction and to vary in the axial direction, the outer body and jet exhaust flows must realign themselves such that, at any axial location, the pressures along the boundaries of the two flows are equal. Korst[10] was able to obtain a unique solution of the base flowfield by

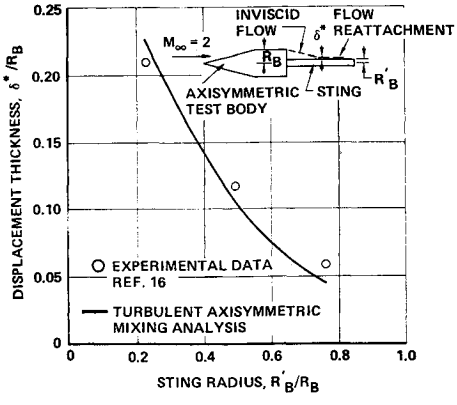

Fig. 6 Reattachment displacement thickness.

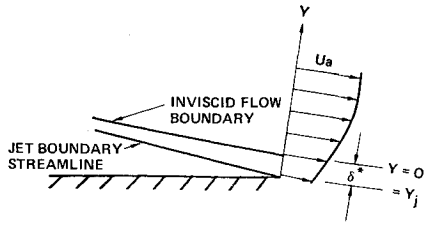

Fig. 7 Mixing layer displacement thickness at reattachment.

postulating an escape criterion for the recompression region in which a discriminating streamline is defined as the one that separates the flow having sufficient energy to accomplish the recompression into region 4-4′ (see Fig. 1) from the flow that does not, and therefore, must recirculate. For this analysis, the Goethert[26] modification of Korst's escape criterion is used; if the $M < 1$ along the discriminating streamline, the flow stagnates and regains its total pressure, which is just sufficient to match the static pressure at region 4-4′; if $M > 1$ along the discriminating streamline, the flow first passes through the equivalent of a normal shock and then regains its total pressure as it stagnates into region 4-4′.

For the back step problem with no bleed into or out of the base region, the discriminating streamline and the jet boundary streamline are identical. However, this is generally not the case for the single-nozzle base flow problem. Usually the flow conditions in the exhaust jet differ from those in the outer body, so that there is a net mass bleed from one stream to the other.

Solution

The solution of the base flow is obtained by requiring the mass in the base region to satisfy continuity. In general form,

$$\int_j^d 2\pi\rho u R dY + \int_{j'}^{d'} 2\pi\rho u R' dY' + G_B = 0 \tag{13}$$

where G_B is the bleed rate into (positive) or out of (negative) the base region (Fig. 5). In terms of η, and employing the relationship,

$$\rho_a u_a(1 - C_a^2) = [2\gamma g_c/(\gamma - 1)\mathcal{R}T_{oa}]^{1/2}P_bC_a$$

Eq. (13) becomes

$$\frac{2\pi R_B\bar{x}P_bC_a}{R_o\sigma}\left(\frac{2\gamma g_c}{(\gamma - 1)\mathcal{R}T_{oa}}\right)^{1/2}\int_{\eta_j}^{\eta_d}\frac{\phi R}{T_o/T_{oa} - C_a^2\phi^2}\,d\eta + \frac{2\pi R'_B\bar{x}'P_bC'_a}{R'_o\sigma'}\left(\frac{2\gamma' g_c}{(\gamma' - 1)\mathcal{R}'T'_{oa}}\right)^{1/2}\times \int_{\eta'_j}^{\eta'_d}\frac{\phi' R'}{T'_o/T'_{oa} - C'^2_a\phi'^2}\,d\eta' + G_B = 0 \tag{14}$$

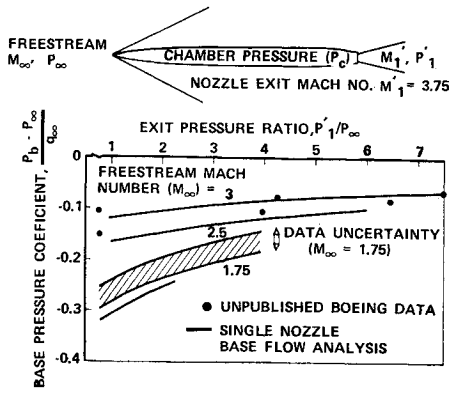

Fig. 8 Base pressure coefficients, cold air exhaust.

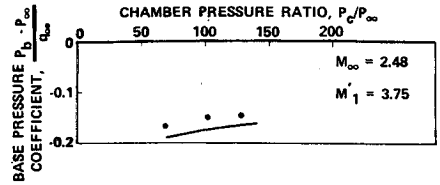

Fig. 9 Base pressure coefficients, cold methane exhaust.

Equation (14) is solved by iterating on P_b until the equation is satisfied. The flow conditions in regions 1 and 1′ (see Fig. 1) must be known, as well as the base geometry. Then, by specifying P_b, the inviscid flowfield from regions 1 to 3 is computed. The plume flowfield from regions 1′ to 3′ is computed using the pressure distribution computed for the outer flow as a boundary condition. The flow direction along the slip line in region 4-4′ is iterated until $P_4 = P'_4$. With the complete solution for the inviscid flowfield, the mixing layer parameters η_m, η_j, and η_d are determined for both the body and jet exhaust flowfields; Eq. (14) is then solved for G_B. This procedure is repeated until the desired value of G_B is achieved.

Evaluating the mixing layer parameters for the solution of Eq. (14) requires the specification of X and X'. The appropriate location for the mixing layer calculation is at the point where the discriminating streamlines from the outer and jet plume flows intersect. In practice, this would increase greatly the time required to obtain a solution. In separate calculations, it was found that the discriminating streamlines intersect at a point where X and X' are equal to approximately 0.8 of the value obtained from the inviscid flow intercepts. This value was used for all the results presented in this paper.

Results

Since numerous papers adequately support Korst's formulation of the base flow theory, this paper contains only data pertaining to the application of this theory to axisymmetric flows. An important element of the present analysis is the extension of two-dimensional mixing to axisymmetric flow. No detailed measurements of the mixing layer were found for the base flows considered in the present analysis, so that no direct comparisons could be made. However, data such as that presented in Fig. 2 permit the inference of mixing layer data that can be used to give credence to the analysis. The inviscid flow boundary in Fig. 2 is displaced from the sting surface. In the reattachment region, this displacement is due to the viscous effects in the reattaching mixing layer. As in boundary-layer flows, a displacement thickness δ^* can be defined that effectively displaces the inviscid flow due to viscous effects (Fig. 6); it is the distance between the inviscid flow boundary and the body sting measured normal to the flow boundary in the reattachment region (Fig. 7). As indicated previously, the inviscid flow boundary presented in Fig. 2 was determined by the method of characteristics, using the measured $P(X)$ in the base region as the boundary condition.

The δ^* points inferred from Fig. 2 are shown in Fig. 6 (along with the curve computed from the mixing analysis); they were determined for the point where the discriminating streamline intercepted the sting, $\delta^* = -Y_d$. The experimental data were obtained for zero mass bleed, so that $Y_d = Y_j$. The good agreement obtained between theory and experiment gives credence to the validity of the axisymmetric mixing analysis.

Although the analysis reported in this paper describes the complete base flowfield, the primary purpose for its formulation was for the prediction of base drag. The real test of its validity, therefore, is the agreement obtained for P_b. Comparison of the results with data obtained in the Boeing Supersonic Wind Tunnel on a slender boattailed body are shown in Figs. 8 and 9. Cold air was used to simulate the hot exhaust flow in most of the tests. The test model was supported by a strut, which had an influence on the flowfield. Small corrections, deduced from tests with image struts, were applied to the data for M_∞'s of 2.5 and 3. Large corrections were applied at Mach 1.75. Considerable uncertainty is associated, therefore, with the latter data; a band equivalent to about 17% is indicated in Fig. 8 rather than data points. Correlation of the data indicates improved agreement with increasing M_∞ or increasing P_c (or exit pressure). Figure 9 presents data obtained using cold methane to obtain a better simulation of hot exhaust gases; the chamber pressure ratios shown are roughly equivalent to the low end of the exit pressure ratios shown in Fig. 8.

In Fig. 10, the analysis is compared to data obtained on cylindrical bodies[6,27] tested at $M_\infty = 2$ and $M_\infty = 3.21$. The figure presents the ratio of base to body static pressure, P_b/P_c, vs the ratio of jet to body total pressure, $P_c/P_{o\infty}$, for

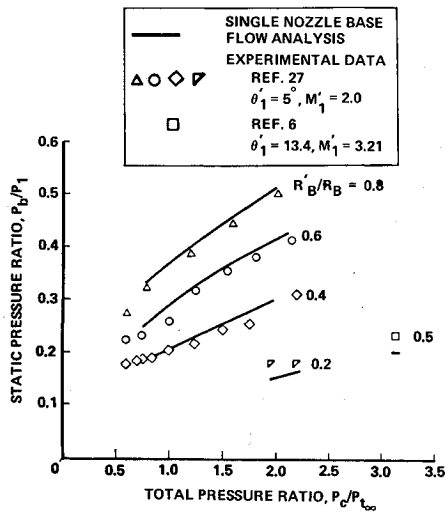

Fig. 10 Base pressure on a cylindrical model.

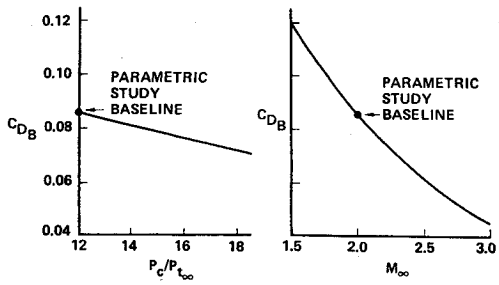

Fig. 11 Effects of exhaust-jet total pressure and free-stream Mach number on base drag.

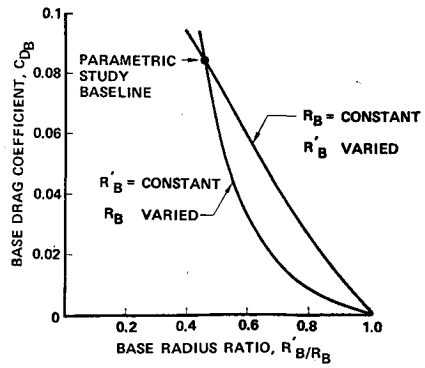

Fig. 12 Effect of base geometry on base drag.

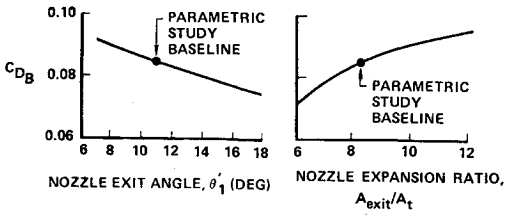

Fig. 13 Effects of nozzle exit angle and nozzle expansion ratio on base drag.

various jet/body radius ratios. Both the experimental data and the theoretical analysis show that P_b is significantly affected by all of these parameters. Good agreement is obtained between the analysis and experiment even when $R'_B/R_B \ll 1$, a real test of the analysis, because axisymmetric effects have their largest impact for this condition.

Parametric Study

A parametric study was performed by applying the theoretical analysis to a slender, axisymmetric body with a single supersonic exhaust nozzle (the baseline vehicle), similar to the test vehicle used to obtain the data presented in Figs. 8 and 9. The results obtained for the base drag coefficient are shown in Figs. 11–14.

Figure 11 shows that increasing P_c results in an increase in jet exit pressure P'_1, which increases P_b, thereby reducing C_{D_B}. Increasing M_∞ decreases both P_b and C_{D_B}. This apparent inconsistency results from the effect of q_∞ in the definition of C_{D_B},

$$C_{D_B} = (P_\infty - P_b)A_B/q_\infty A_{ref}$$

The pressure increment, $P_\infty - P_b$, increases as M_∞ is increased and P_b falls, but $q_\infty = P_\infty\gamma_\infty M_\infty^2/2$ increases faster than $P_\infty - P_b$, so that C_{D_B} is reduced.

Increasing R'_B/R_B reduces C_{D_B} as shown in Fig. 12, because A_B is reduced and P_b is increased (for given θ'_1 and ϵ). The most effective means of increasing R'_B/R_B is seen to depend on its value.

Increasing the nozzle exit angle θ'_1 and decreasing its expansion ratio ($\epsilon = A'_1/A_t$) results in a decrease in C_{D_B} (Fig. 13). Increasing θ' increases the pressure at reattachment, which causes P_b to be increased; therefore, C_{D_B} is reduced. In the calculations performed for the ϵ effect, P_c was fixed. Decreasing ϵ results in an increase of P'_1, so that P_b is increased, and C_{D_B} is reduced. The effects of boattail angle θ_1 on the afterbody and base drags is shown in Fig. 14. For small $\theta_1 < 4°$, increasing θ_1 (for given length) is an effective means of reducing C_{D_B} by reducing A_B. For $\theta_1 > 4°$, the effect of θ_1 on C_{D_B} is small, but the afterbody pressure drag continues to rise, so that the overall drag increases. Thus, a minimum-total-drag configuration is not necessarily a minimum-base-drag configuration.

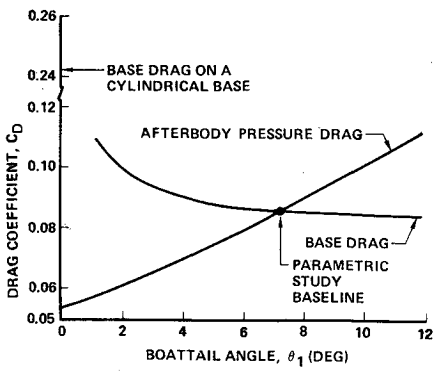

Fig. 14 Effect of boattail angle on afterbody drag.

Conclusion

Turbulent base flow theory involves the analysis of separate flow components and the simultaneous solution of the resulting analyses to obtain the final solution for the base flowfield. Each of the separate flow components is complex and has been simplified in the present analysis. These simplifications appear to be reasonable, and the results agree rather well with experimental data. The analysis is capable of further refinement by considering the effects of mixing region initial boundary layers and pressure gradients, and improved realignment criterion.[28] The development of this analysis could have been assisted with detailed experimental data on bodies with a jet exhausting from the base; such data are not available. Considering the potential impact of the afterbody design on flight vehicle performance, and the costs, problems, and time delays involved in developmental testing, it would seem that the acquisition of basic experimental data of this nature would be a significant contribution.

References

[1] Sedney, R., "Review of Base Drag," *The Fluid Dynamic Aspects of Ballistics, AGARD Conference Proceedings No. 10,* Sept. 1966, pp. 211–240.

[2] Przirembel, C. E. G. and Page, R. H., "Analysis of Axisymmetric Supersonic Turbulent Base Flow," *Proceedings of the 1968 Heat Transfer and Fluid Mechanics Institute,* Stanford Univ. Press, 1968, pp. 258–272.

[3] Hong, Y. S., "A Study of Axially-Symmetric Supersonic Base Flow with Turbulent Initial Boundary Layer," Ph.D. thesis, 1968, Dept. of Mechanical Engineering, Univ. of Washington, Seattle, Wash.

[4] Redeker, E., "Summary of References Containing Base Drag Data on Single Nozzle Missile Configurations," D2-125621-1, 1968, Boeing Company, Seattle, Wash.

[5] Boughman, E. L. and Kochendorfer, F. D., "Jet Effects on Base Pressures of Conical Afterbodies at Mach 1.91 and 3.12," RM E57E06, 1957, NACA.

[6] Beheim, M. A., Klann, J. L., and Yeager, R. A., "Jet Effects on Annular Base Pressure and Temperature in a Supersonic Stream," TR R-125, 1962, NASA.

[7] Korst, H. H., "A Theory for Base Pressures in Transonic and Supersonic Flow," *Transactions of the ASME: Journal of Applied Mechanics* (Vol. 23), Vol. 78, 1956, pp. 593–600.

[8] Korst, H. H. and Tripp, W., "The Pressure on a Blunt Trailing Edge Separating Two Supersonic Two-Dimensional Air Streams of Different Mach Numbers and Stagnation Pressures, but Identical Stagnation Temperatures," *Proceedings of the Fifth Midwestern Conference on Fluid Mechanics,* Univ. of Michigan, Ann Arbor, Mich., 1957, pp. 187-199.

[9] Kessler, T. J., "A Theory for Two Dimensional Supersonic Turbulent Base Flows," AIAA Paper 69-68, New York, 1969.

[10] Korst, H. H., Chow, W. L., and Zumwalt, G. W., "Final Report on Research on Transonic and Supersonic Flow of a Real Fluid at Abrupt Increases in Cross Section (With Special Consideration of Base Drag Problems)," ME-TR-392-5, OSR-TR-60-74, Contract AF18(600)-392, 1959, Univ. of Illinois, Urbana, Ill.

[11] Street, T. A., "Base Pressure Program for a Body of Revolution with Nozzle Flow," Rept. RF-TM-64-2, 1964, U.S. Army Missile Command, Redstone Arsenal, Ala.

[12] Eastman, D. W., "Two Dimensional or Axially Symmetric Real Gas Flows by the Method of Characteristics, Part I: Formulation of the Equations," D2-10597, 1961, Boeing Company, Seattle, Wash.

[13] Eastman, D. W., "Two Dimensional or Axially Symmetric Real Gas Flows by the Method of Characteristics, Part II: Flow Fields Around Bodies," D2-10598, 1963, The Boeing Co., Seattle, Wash.

[14] Eastman, D. W., "Two Dimensional or Axially Symmetric Real Gas Flows by the Method of Characteristics, Part III: A Summary of Results from the IBM 7090 Program for Calculating the Flow Field of a Supersonic Jet," D2-10599, 1962, The Boeing Co., Seattle, Wash.

[15] Hausen, C. F., "Approximations for the Thermodynamics and Transport Properties of High Temperature Air," TR R-50, 1959, NASA.

[16] Beheim, M. A., "Flow in the Base Region of Axisymmetric and Two Dimensional Configurations," TR R-77, 1960, NASA.

[17] Love, E. S., "Base Pressure at Supersonic Speeds on Two-Dimensional Airfoils and on Bodies of Revolution with and without Fins Having Turbulent Boundary Layers," TN-3819, Jan. 1957, NACA.

[18] Sieling, W. R., "The Effect of Sting Diameter and Length on Base Pressure at M = 3.88," *The Aeronautical Quarterly*, Vol. 19, No. 4, 1968, pp. 368–374.

[19] Page, R. H. and Korst, H. H., "Nonisoenergetic Turbulent Compressible Jet Mixing with Consideration of its Influence on the Base Pressure Problem," *Proceedings of the Fourth Midwestern Conference on Fluid Mechanics*, Purdue Univ., Sept. 1955, pp. 45–68.

[20] Lamb, J. P., "An Approximate Theory for Developing Turbulent Free Shear Layers," *Transactions of the ASME, Ser. D: Journal of Basic Engineering*, Vol. 89, 1967, pp. 633–642.

[21] Korst, H. H., Page, R. H., and Childs, M. E., "A Theory for Base Pressures in Transonic and Supersonic Flow," ME TN 392-2, OSR TN 55-39, 1955, Univ. of Illinois, Engineering Experiment Station.

[22] Vasiliu, J., "Turbulent Mixing of a Rocket Exhaust Jet with a Supersonic Stream, Including Chemical Reactions," *Journal of the Aerospace Sciences*, Vol. 29, No. 1, Jan. 1962, pp. 19–28.

[23] Page, R. H. and Dixon, R. J., "Computer Evaluation of an Integral Treatment of Gas Mixing," *Proceedings of the Third Conference on Performance of High Temperature Systems, Dec. 1964, Pasadena, Calif.*, Gordon and Breach, New York, 1969, pp. 345–370.

[24] Korst, H. H., Page, R. H., and Childs, M. E., "Compressible Two-Dimensional Jet Mixing at Constant Pressure," ME-TN-392-1, April 1954, Univ. of Illinois, Engineering Experiment Station.

[25] Pai, S. I., *Viscous Flow Theory—Laminar Flow*, Van Nostrand, Princeton, N. J., 1956, pp. 262–263.

[26] Goethert, B. H., "Base Flow Characteristics of Missiles with Cluster-Rocket Exhausts," Paper 69-89, July 1960, IAS.

[27] Reid, J. and Hastings, R. C., "The Effect of a Central Jet on the Base Pressure of a Cylindrical Afterbody in a Supersonic Stream," RM 3224, 1959, Royal Aircraft Establishment.

[28] Page, R. H., Kessler, T. J., and Hill, W. G., Jr., "Reattachment of Two-Dimensional Supersonic Turbulent Flows," Paper 67-FE-20, 1967, ASME.

JULY 1970 J. SPACECRAFT VOL. 7. NO. 7

A Thin Strap Support for the Measurement of the Dynamic Stability Characteristics of High-Fineness-Ratio, Wind-Tunnel Models

W. A. MILLARD* AND W. H. CURRY†
Sandia Laboratories, Albuquerque, N. M.

A transverse support system that appears to have minimal support interference effects has been developed for use in dynamic stability tests of high- fineness ratio, wind-tunnel models. A thin metal strap is placed in tension between the walls of the tunnel, and the model is mounted on it in a manner which allows the model to oscillate freely in the plane of the strap. Dynamic stability tests using this rig were conducted at Mach number 7.3 on a model of the Tomahawk rocket, which has a fineness ratio of 23.3. The test results correlate reasonably well with data derived from theoretical studies, from other wind-tunnel programs, and from full-scale flight test.

Nomenclature

$C_m, C_{m\alpha}$ = pitching moment coefficient and slope
$C_{mq} + C_{m\dot{\alpha}}$ = damping moment coefficient (based on $d/2V$)
$C_N, C_{N\alpha}$ = normal force coefficient and slope
d = maximum body diameter and reference length
M = Mach number
Re = Reynolds number based on body length
S = body cross-sectional area and reference area
V = velocity
α = angle of attack
ϕ = angle of roll (zero when fins in + position)

Presented as Paper 69-350 at the AIAA 4th Aerodynamic Testing Conference, Cincinnati, Ohio, April 28–30, 1969; submitted May 21, 1969, revision received January 26, 1970. This work was supported by the United States Atomic Energy Commission. The concept of the strap rig was introduced by G. W. Stone, Sandia Laboratories. The authors wish to thank G. W. Stone for his assistance in planning and conducting the test program, and R. D. Fellerhoff for the design of the test hardware. The authors also wish to thank A. R. Wallace of ARO Inc. for his technical assistance during the wind-tunnel free flight test at Arnold Engineering Development Center which is described in the Appendix.

* Staff Member, Rocket and Recovery Systems Division, Aerothermodynamics Projects Department. Member AIAA.

† Supervisor, Experimental Aerodynamics Division, Aerothermodynamics Project Department. Associate Fellow AIAA.

Introduction

The measurement of the dynamic stability characteristics of high-fineness-ratio shapes in a wind tunnel by means of the free oscillation technique using a fixed support has long been a problem. A sting supporting the model will in general not allow sufficient oscillation amplitude. A transverse support system interferes with the flowfield over the model. The type of transverse support generally used is a rod installed perpendicular to the model's plane of oscillation. Interference effects in this case could be significant on the aftersection of a finned model oscillating through the support wake.

A transverse support system that appears to have minimal support interference is a strap placed in tension in the pitch plane of the model (Fig. 1). Because the strap is not subjected to large bending loads, it can be made extremely thin, and its wake will be small. This report describes the test apparatus and presents the results of an investigation of the dynamic stability characteristics of a model of the Tomahawk sounding rocket.